Activation of the Nrf2/HO-1 signaling pathway contributes to the protective effects of coptisine against oxidative stress-induced DNA damage and apoptosis in HaCaT keratinocytes

Yung Hyun Choi[1,2]

[1] *Department of Biochemistry, Dong-eui University College of Korean Medicine, Busan, Republic of Korea*
[2] *Anti-Aging Research Center, Dong-eui University, Busan, Republic of Korea*

Abstract. In this study, the protective effect of coptisine on the oxidative damage-mediated apoptosis was evaluated in cultured human HaCaT keratinocytes. The results demonstrate that preincubation of cells with coptisine prior to H_2O_2 stimulation resulted in significant inhibition of cytotoxicity and DNA damage associated with the inhibition of reactive oxygen species (ROS) accumulation. Coptisine also restored H_2O_2-induced mitochondrial dysfunction and decrease of ATP production, and prevented apoptosis by inhibiting Bax/Bcl-2 ratio, caspase-3 activity, and poly(ADP-ribose) polymerase degradation. Interestingly, the expressions of nuclear factor-erythroid-2-related factor 2 (Nrf2) and its active form, phosphorylated Nrf2, were strikingly promoted by coptisine in the presence of H_2O_2, which was associated with a marked increase in the expression of heme oxygenase-1 (HO-1). However, coptisine-induced HO-1 expression was completely abrogated by Nrf2-specific small interfering RNA (Nrf2-siRNA), which suggests that the increased expression of HO-1 by coptisine is Nrf2-dependent. In addition, Nrf2-siRNA transfection significantly eliminated the protective effect of coptisine on H_2O_2-induced cytotoxicity, and this effect was similar to that by zinc protoporphyrin IX (ZnPP), an HO-1 specific inhibitor. Furthermore, the protective effects of coptisine against H_2O_2-induced cytotoxicity were abolished by ZnPP, indicating that coptisine protects keratinocytes against oxidative stress-induced injury through activation of the Nrf2/HO-1 signaling pathway.

Key words: Coptisine — Keratinocytes — ROS — DNA damage — Apoptosis — Nrf2/HO-1

Introduction

While adequate levels of reactive oxygen species (ROS) act as signaling molecules to maintain normal cellular function, excessive ROS production due to balance disturbances between pro-oxidant and antioxidant systems causes oxidative damage to most tissues (Valko et al. 2016; Treberg et al. 2019). In particular, ROS was found to be crucially involved in the induction of DNA damage and cell death by ultraviolet B (UVB) irradiation in skin cells (Kulms and Schwarz 2002; D'Errico et al. 2007). Among the intracellular organelles, mitochondria are the major source of ROS

production in keratinocytes exposed to UVB, and are the most vulnerable targets of ROS (Piao et al. 2012; Rezvani et al. 2007). Moreover, the accumulation of ROS beyond the antioxidant function of cells could reduce mitochondrial membrane potential (MMP), an index of the electron transport chain performance, resulting in compromised ATP production (Rigoulet et al. 2011; Sosa et al. 2013). Subsequently, apoptogenic proteins, including cytochrome *c*, are released from the mitochondrial intermembrane space into the cytoplasm, and play a central role in an induction signal for apoptosis (Finkel and Holbrook 2000; Rigoulet et al. 2011). Therefore, supplementation of antioxidants has been proposed as a strategy to prevent ROS generation through the activation of signaling pathways that inhibit free radical accumulation.

Coptisine is a naturally occurring isoquinoline alkaloid compound with a similar parent structure to berberine de-

Correspondence to: Yung Hyun Choi, Department of Biochemistry, Dong-eui University College of Korean Medicine, 52-57, Yangjeong-ro, Busanjin, Busan 47227, Republic of Korea
E-mail: choiyh@deu.ac.kr

rived from Coptidis Rhizoma, the roots of *Coptis chinensis* Franch, which has been widely used in traditional medicine for the treatment of a number of diseases (Xu et al. 2017; Meng et al. 2018). Many previous studies have shown that this compound has beneficial multi-pharmacological effects, including antioxidant activity (Cho et al. 2004; Yokozawa et al. 2004; Jang et al. 2009; Jung et al. 2009). For example, Coptidis Rhizoma alkaloids, including coptisine, have been reported to protect DNA damage by nitric oxide (NO)-agonist drug in renal tubular epithelial cells by blocking peroxynitrite ($ONOO^-$) formation (Yokozawa et al. 2004), which suggests that coptisine may be useful for the development of pharmacological agents for the treatment of disorders associated with oxidative stress. In addition, coptisine has been shown to improve cardiac systolic and diastolic dysfunction, and to ameliorate mitochondrial respiratory dysfunction by high doses of isoproterenol, a synthetic catecholamine and β-adrenergic agonist, due to its strong antioxidant activity (Gong et al. 2012). Moreover, recent studies have shown that coptisine acts as a powerful ROS scavenger through activating the nuclear factor-erythroid-2-related factor 2 (Nrf2) signaling pathway, and can effectively exacerbate oxidative stress (Hu et al. 2017; Luo et al. 2018). These antioxidant defense effects of Nrf2 signal transduction by coptisine seem to play an important role in regulating cell proliferation and apoptosis. Zinc protoporphyrin IX (ZnPP), on the other hand, is a type of metalloporphyrins found in red blood cells when heme production is suppressed (Cheng et al. 2012; Kuribayashi et al. 2015). ZnPP competitively suppresses the activity of heme oxygenase-1 (HO-1), one of the major genes regulated by Nrf2, due to its similarity to heme in the porphyrin loop structure, and reduce bilirubin production rates. Due to this characteristic, ZnPP is widely used as a blocker of HO-1 activity (Fang et al. 2009; Hjortsø and Andersen 2014). However, no studies have been reported on the protective effect of coptisine against oxidative stress in skin cells. The aim of this study was to explore the usefulness of coptisine as part of a program to find defensive substances against oxidative stress (hydrogen peroxide, H_2O_2) in cultured HaCaT human skin keratinocytes.

Materials and Methods

Cell culture and coptisine treatment

HaCaT keratinocyte cell line was obtained from the American Type Culture Collection (Manassas, MD, USA), and maintained in RPMI 1640 medium (WelGENE Inc., Daegu, Republic of Korea) containing 10% (v/v) heat-inactivated fetal bovine serum (WelGENE Inc.), streptomycin (100 μg/ml), and penicillin (100 Units/ml) at 37°C in a humidified atmosphere containing 5% CO_2 and 95% air. Coptisine ($C_{19}H_{14}NO_4^+$, purity ≥ 98%), which was purchased from Sigma-Aldrich Chemical Co. (St. Louis, MO, USA), was dissolved in dimethyl sulfoxide (DMSO, Sigma-Aldrich Chemical Co.), and diluted with cell culture medium to adjust the final treatment concentrations, prior to use in the experiments. For the cell viability study, HaCaT cells were treated with different concentrations of coptisine for 24 h, or pretreated with coptisine for 1 h, before H_2O_2 (0.5 mM, Sigma-Aldrich Chemical Co.) treatment for 24 h. The cells were also treated with 10 μM ZnPP (Sigma-Aldrich Chemical Co.), a well established HO-1 inhibitor, for 1 h in the presence or absence of H_2O_2.

Cell viability assay

After completion of treatment, the medium was removed, and 0.5 mg/ml of 3-(4,5-dimethylthiazol-2-yl)-2,5-diphenyltetrazolium bromide (MTT, Sigma-Aldrich Chemical Co.) was added to each well, and incubated at 37°C for 3 h. The supernatant was then replaced with an equal volume of DMSO to dissolve the blue formazan crystals for 10 min. Optical density was measured at a wavelength of 540 nm with a microplate reader (Dynatech Laboratories, Chantilly, VA, USA). All experiments were performed in triplicate, and the results were expressed as the percentage of MTT reduction, assuming that the absorbance of control was 100%.

Small interfering RNA (siRNA) transfection

siRNA-mediated silencing of the Nrf2 gene was performed using siRNA duplexes purchased from Santa Cruz Biotechnology, Inc. (Santa Cruz, CA, USA). In brief, the HaCaT cells were seeded (1×10^4 cells/ml) in 6-well culture plates, and Nrf2-siRNAs and control siNRAs were transfected into the cells using the Lipofectamine™ 2000 reagent (Life Technologies, Carlsbad, CA, USA), according to the manufacturer's instructions. The transfected cells were pretreated with or without coptisine and/or ZnPP for 1 h, before adding H_2O_2 for a further 24 h.

Western blot analysis

After being subjected to the necessary experimental treatments, the cells were harvested, washed with phosphate buffered saline (PBS), and lysed with lysis buffer for 30 min to extract whole-cell proteins, as described in the previous study (Kim et al. 2018). Protein concentrations were quantified using a Bio-Rad protein analysis kit (Bio-Rad Lab., Hercules, CA, USA), and the equal amounts (40 μg) of protein samples were subjected to sodium dodecyl sulfate-polyacrylamide (SDS)-gel electrophoresis, and then

transferred onto polyvinylidene fluoride membranes (Millipore, Bedford, MA, USA). Membranes were blocked with 5% bovine serum albumin (Sigma-Aldrich Chemical Co.) for 1 h in a mixture of Tris-Buffered Saline and Tween-20 (TBST), and probed with primary antibodies overnight at 4°C. The primary antibodies against Nrf2, Keap1, poly(ADP-ribose) polymerase (PARP), Bax, Bcl-2 and caspase-3 were purchased from Santa Cruz Biotechnology, Inc. (Dallas, TX, USA). Antibody for phosphor (p)-Nrf2 was obtained Abcam, Inc. (Cambridge, UK). The primary antibodies against histone variant H2A.X (γH2A.X) and p-γH2A.X were purchased from Cell signaling Technology (Danvers, MA, USA). Anti-HO-1 and anti-actin antibodies were obtained from Calbiochem-Novabiochem Co. (San Diego, CA, USA) and Bioworld Technology, Inc. (St Louis Park, MN, USA), respectively. The membranes were then incubated with the appropriate secondary antibodies conjugated with horseradish peroxidase (Santa Cruz Biotechnology, Inc.) for 2 h at room temperature, and rinsed three times with TBST. The protein bands were visualized by incubating the membranes in an enhanced chemiluminescence (ECL) reagent (Amersham Biosciences, Westborough, MA, USA), according to the manufacturer's instructions. The immunoreactive bands were detected and exposed to X-ray film. Images of Western blotting were also analyzed using ImageJ (Vilber Lourmat, Torcy, France).

Measurement of ROS

Intracellular ROS levels were assessed by staining cells using the oxidation-sensitive dye 2′,7′-dichlorofluorescein diacetate (DCF-DA). In brief, cells were washed twice with cold PBS, suspended in PBS, and stained with 10 μM DCF-DA (Sigma-Aldrich Chemical Co.) for 20 min at 37°C in the dark. Relative fluorescence intensities of cell suspensions were measured using a flow cytometer (Becton Dickinson, San Jose, CA, USA). To assess intracellular ROS production by image analysis, cells were seeded on a coverslip loaded 6-well plate for 24 h, treated with coptisine and/or ZnPP for 1 h, and then with H_2O_2 for 1 h. After washing with PBS, cells were stained with 10 μM DCF-DA for 20 min at 37°C, washed, and mounted on microscope slides using mounting medium (Sigma-Aldrich Chemical Co.). The images were obtained using a fluorescence microscope (Carl Zeiss, Oberkochen, Germany).

Comet assay for DNA damage

DNA damage in individual cells was assessed using an alkaline comet assay, as previously described (Park et al. 2018). Cells were seeded on 6-well plates at a density of 3×10^5 cells/well for 24 h, and treated with or without coptisine and/or ZnPP for 1 h, before adding H_2O_2 for

a further 24 h. The cells were detached from culture surfaces, mixed with 0.75% low-melting agarose (LMA), and transferred to a microscope slide precoated with a layer of 0.75% normal-melting agarose. After solidification, slides were covered with LMA, and immersed in lysis solution (2.5 M NaCl, 100 mM Na-ethylenediaminetetraacetic acid (EDTA), 10 mM Tris, 1% Triton X-100, and 10% DMSO (pH 10)) for 1 h at 4°C to remove proteins. The slides were then placed in a horizontal electrophoresis tank containing electrophoresis buffer (300 mM NaOH, 10 mM Na-EDTA, pH 10) for 20 min, to allow DNA unwinding under alkaline/neutral conditions. Thereafter, electrophoresis was conducted in the same buffer for 20 min at 4°C, to draw negatively-charged DNA towards the anode. Slides were then rinsed gently three times with neutralization buffer (0.4 M Tris-HCl, pH 7.5) for 10 min at 25°C, stained with ethidium bromide (EtBr, 10 μg/ml, Sigma-Aldrich Chemical Co.), and observed under a fluorescence microscope. All of the steps above were conducted under yellow light to prevent DNA damage.

Determination of 8-hydroxy-2′-deoxyguanosine (8-OHdG)

The BIOXYTECH® 8-OHdG-EIA™ kit (OXIS Health Products Inc., Portland, OR, USA) was used to quantify oxidative DNA damage. Briefly, cells were pretreated with or without coptisine and/or ZnPP for 1 h, prior to treatment with H_2O_2 in the presence or absence of coptisine. After 24 h culture, cellular DNA was isolated using a DNA extraction kit (iNtRON Biotechnology Inc., Sungnam, Republic of Korea), and quantified according to the manufacturer's protocol. The amount of 8-OHdG, a deoxyriboside form of 8-oxoguanine, in DNA was found using a standard curve by measuring the absorbance at 450 nm, using a microplate reader according to the manufacturer's instructions.

Measurement of MMPs (ΔΨm)

To assess MMP losses, cells were collected after respective treatments, and incubated in media containing 10 μM of JC-1 (5,5'6,6'-tetrachloro-1,1',3,3'-tetraethyl-imidacarbocyanine iodide; Sigma-Aldrich Chemical Co.), a mitochondria-specific fluorescent dye, for 20 min at 37°C in the dark. After washing twice with PBS to remove unbound dye, green (JC-1 monomers) to red (JC-1 aggregates) fluorescence ratios were determined by flow cytometer, according to the manufacturer's instructions.

Determination of ATP levels

Intracellular ATP levels were determined using a firefly-luciferase-based ATP Bioluminescence Assay Kit (Roche Applied Science, Indianapolis, IN, USA). Briefly, cells cultured

under various conditions were lysed with the provided lysis buffer, and collected supernatants were mixed with an equal amount of luciferase agent, which catalyzed the reaction between ATP and luciferin. Emitted light was immediately measured using a microplate luminometer, and ATP levels were calculated using a standard curve.

Colorimetric assay of caspase-3 activity

Caspase-3 activity was assessed using a colorimetric assay kit (R&D Systems, Minneapolis, MN, USA). In brief, the collected cells were lysed, and equal amounts of proteins were incubated with the supplied reaction buffer, which contained the caspase-3 substrates dithiothreitol and tetra-peptides (Asp-Glu-Val-Asp(DEAD)-p-nitroaniline (pNA)), for 2 h at 37°C in the dark. Changes in absorbance at 405 nm were determined using a microplate reader, according to the manufacturer's instructions. Results are presented as multiples of untreated control cell values.

Apoptosis assay using a fluorescence microscope

Apoptosis induction was evaluated by observing nuclear morphological changes. After treating cells with H_2O_2 in the presence or absence of coptisine and/or ZnPP, the cells were harvested, washed with PBS, and then fixed with 4% paraformaldehyde (Sigma-Aldrich Chemical Co.) in PBS for 30 min at room temperature. Cells were then permeabilized with 0.1% (w/v) Triton X-100 for 5 min, stained with 1.0 mg/ml of 4,6-diamidino-2-phenylindole (DAPI, Sigma-Aldrich Chemical Co.) solution for 10 min at room temperature in the dark, and washed twice with PBS. Nuclear morphologic changes were examined using a fluorescence microscope.

Apoptosis analysis using a flow cytometer

Apoptosis extents were determined by flow cytometry using Annexin V/propidium iodide (PI) double staining. In brief, cells were collected, rinsed with PBS, re-suspended in binding buffer, and stained with fluorescein isothiocyanate (FITC)-conjugated annexin V and PI (BD Pharmingen, San Diego, CA, USA) at room temperature for 20 min in the dark, according to the manufacturer's instructions. Cell fluorescence intensities were detected using a flow cytometer, and data were analyzed using Cell Quest Pro software. Annexin$^-$/PI$^+$ cells were considered normal, whereas annexin V-FITC$^+$/PI$^-$ and annexin$^+$/PI$^+$ were considered indicators of early and late apoptotic cells, respectively.

Internucleosomal DNA fragmentation assay

The collected cells were dissolved in lysis buffer (10 mM Tris-HCl (pH 7.4), 150 mM NaCl, 5 mM EDTA, 0.5% Triton X-100, and 0.1 mg/ml proteinase K) for 30 min at room temperature. DNA from the supernatant was extracted by chloroform/phenol/isoamyl alcohol (24/25/1, v/v/v), and was precipitated by ethanol. The extracted DNA was then transferred to 1.5% agarose gel containing 0.1 μg/ml EtBr, and electrophoresis was carried out at 70 V. The gel was visualized using a Chemidox (Bio-Rad Lab., Hercules, CA, USA).

Statistical analysis

All experiments were performed at least three times. Data were analyzed using GraphPad Prism software (version 5.03; GraphPad Software, Inc., La Jolla, CA, USA), and expressed as the mean ± standard deviation (SD). Differences between groups were assessed using analysis of variance followed by ANOVA-Tukey's *post hoc* test, and $p < 0.05$ was considered to indicate a statistically significant difference.

Results

Coptisine inhibited H_2O_2-induced cytotoxicity in HaCaT keratinocytes

HaCaT cells were treated with various concentrations of coptisine and H_2O_2 for 24 h, and the MTT assay was performed to establish the experimental conditions. Figure 1A shows that HaCaT cells treated with concentrations of 75 μg/ml or more revealed a significant decrease in cell viability, but no significant change until 50 μg/ml treatment, compared to the control group. Therefore, the concentration range of coptisine was selected to be less than 50 μg/ml to verify antioxidant efficacy. H_2O_2 concentration for oxidative stress induction was selected to be 0.5 mM, which was about 60% survival rate, compared with control cells (data not shown). To evaluate the protective effect of coptisine on H_2O_2-induced cytotoxicity, HaCaT cells were pretreated with 10, 25, and 50 μg/ml coptisine for 1 h before treatment with 0.5 mM H_2O_2, and cultured for 24 h. Figure 1B shows that pretreatment with 25 and 50 μg/ml coptisine significantly restored cell viability, as compared to H_2O_2 alone, in a concentration-dependent manner.

Coptisine activated the Nrf2/HO-1 signaling pathway in HaCaT keratinocytes

To investigate whether the cytoprotective activity of coptisine on H_2O_2 was correlated with the activation of Nrf2 signaling, the effect of coptisine on the expression of Nrf2 and its regulatory genes was determined. The immunoblotting results showed that the expression of Nrf2 protein

A

B
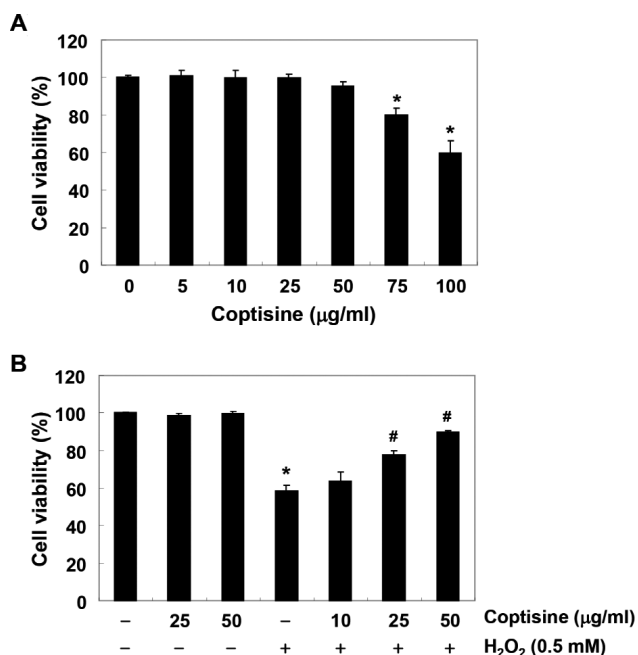
Figure 1. Effects of coptisine on the H_2O_2-induced cytotoxicity in HaCaT cells. Cells were treated with the indicated concentrations of coptisine for 24 h (**A**), or pre-treated with or without coptisine for 1 h, and then stimulated with 0.5 mM H_2O_2 for 24 h (**B**). Cell viability was assessed by MTT reduction assay (* $p < 0.05$ compared with the control group, # $p < 0.05$ compared with the H_2O_2-treated group).

was slightly increased in the H_2O_2 alone group, and more than that in the 50 μg/ml coptisine treated group (Figures 2A and B). However, the expression of Nrf2 protein was markedly increased in H_2O_2-treated cells in the presence of coptisine compared to H_2O_2 and coptisine alone, and the expression of the phosphorylated form of Nrf2 (p-Nrf2, at serine 40), which meant that Nrf2 was activated, was also markedly increased in the co-treatment group. In addition, the increase in coptisine-induced activation of Nrf2 was accompanied by an induction of HO-1 expression, but the expression of Kelch-like ECH associated protein 1 (Keap1) was decreased in a coptisine treatment-dependent manner. Therefore, a loss-of-function experiment using siRNA was performed to investigate whether the increase in HO-1 expression by coptisine is an Nrf2-dependent phenomenon. When transiently transfected with Nrf2 specific siRNA (Nrf2-siRNA), as shown in Figures 2C and D, the increased expression of Nrf2, p-Nrf2, and HO-1 in cells co-treated with coptisine and H_2O_2 was effectively abolished. Consequently, the expression of Keap1 in the cells treated with Nrf2-siRNA was maintained at the control level, which means that the augmentation of HO-1 expression by coptisine is Nrf2-dependent.

The protective effect of coptisine on H_2O_2-induced HaCaT cell cytotoxicity was Nrf2/HO-1 signaling dependent

Next, the relationship between the activation of Nrf2 / HO-1 signaling by coptisine and the protective effect against oxidative stress were determined. As shown in Figure 2E, Nrf2 expression interference significantly eliminated the effect of improving the cell viability of coptisine against H_2O_2 treatment, demonstrating that Nrf2/HO-1 signaling plays a critical role in the coptisine protective effect of H_2O_2-induced oxidative stress in HaCaT cells. It was also found that the protective effect of coptisine was reversed by blocking the activation of HO-1 by ZnPP, a HO-1 selective inhibitor (Figure 2F). These results indicate that Nrf2-mediated HO-1 expression by coptisine in HaCaT cells is an important mediator in inhibiting H_2O_2-induced cytotoxicity.

### Coptisine attenuated H_2O_2-induced ROS generation in HaCaT keratinocytes

The effect of coptisine on the production of ROS by H_2O_2 was examined to further investigate whether the protective effect of coptisine on H_2O_2-induced cytotoxicity was due to the blockade of oxidative stress. For this purpose, the production of ROS was examined using a fluorescent labeled probe, DCF-DA, and the fluorescence intensity was markedly increased within 1 h in the cells exposed to H_2O_2 compared to the control (Figures 3A and B). However, the accumulation of ROS in HaCaT cells pretreated with coptisine was significantly reduced compared to in those with H_2O_2 alone treatment. In addition, the fluorescence microscope observation again confirmed that coptisine had a powerful ROS scavenging effect (Figure 3C). However, the suppression of HO-1 activity by ZnPP offset the inhibitory effect of coptisine on ROS production, indicating that the cytoprotective effects of coptisine on oxidative stress may be mediated by ROS generation blockade through HO-1 activation.

### Coptisine reduced H_2O_2-induced DNA damage in HaCaT keratinocytes

To determine whether coptisine prevents DNA damage, the effect of coptisine on the H_2O_2-induced phosphorylation of γH2AX protein (p-γH2AX, at serine 139), one of the DNA strand break markers, was assessed. The immunoblotting results of Figures 4A and B show that the marked increase in p-γH2AX in H_2O_2-stimulated cells was reduced by pre-treatment with coptisine compared to untreated control cells, without altering the expression of total γH2AX protein. Additionally, in the comet assay, another method for detecting DNA strand breaks, there was no smeared pattern of nuclear DNA in untreated control and coptisine alone treated cells. However, in H_2O_2-stimulated cells, the length of the comet

tail clearly increased, which means DNA damage occurred; and in coptisine pretreated cells, tail length was obviously shorter than in H_2O_2-treated cells (Figure 4C). Furthermore, H_2O_2 treatment significantly increased the production of 8-OHdG adduct, a specific marker of DNA oxidative damage, compared to the control group, but pretreatment of coptisine significantly reduced the production of 8-OHdG by H_2O_2 (Figure 4D). On the other hand, ZnPP excluded
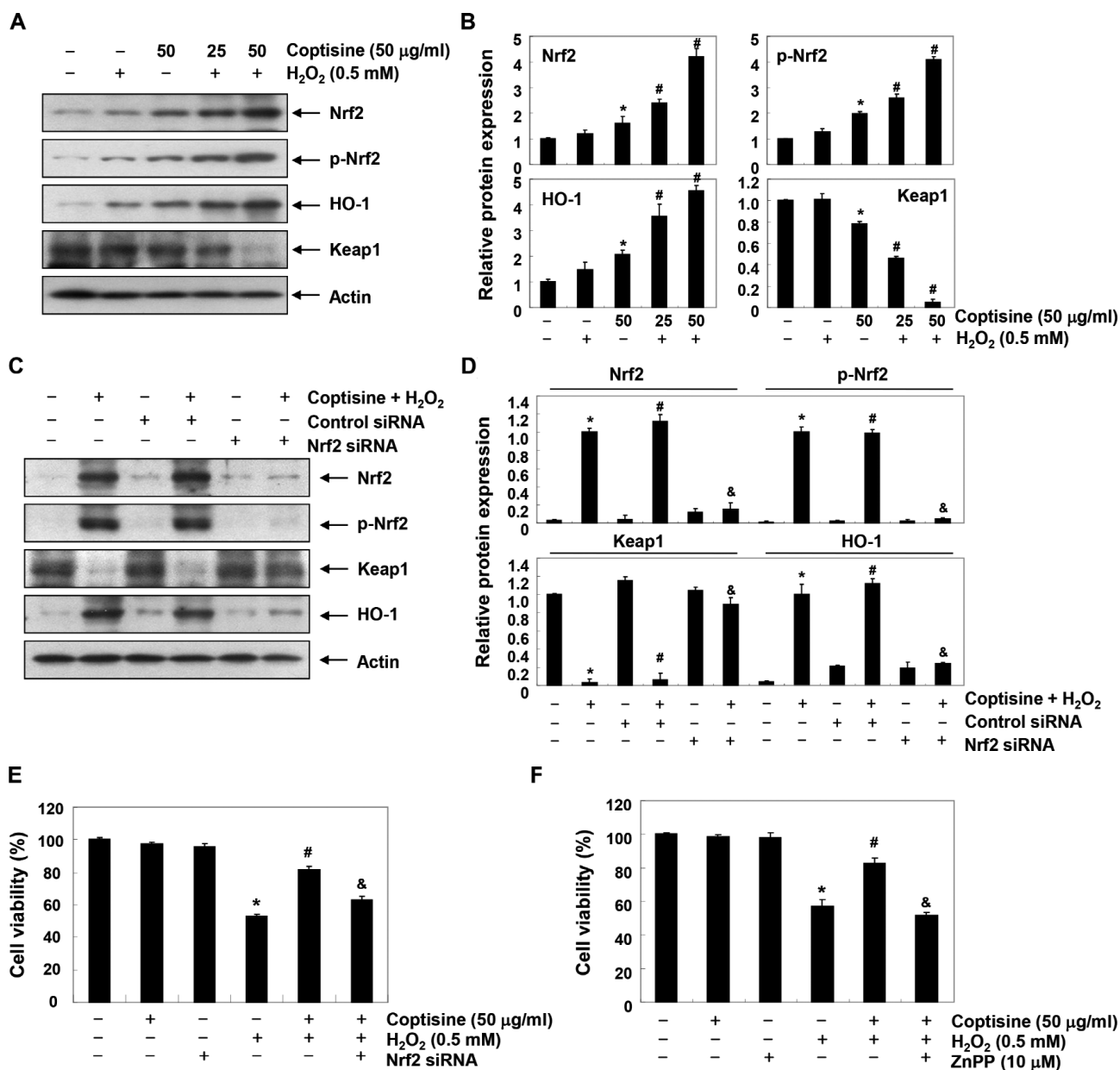
Figure 2. Involvement of Nrf2/HO-1 signaling in the protective effect of coptisine on H_2O_2-induced HaCaT cell cytotoxicity. **A., B.** Cells were pretreated with or without the indicated concentrations of coptisine for 1 h, and then stimulated with 0.5 mM H_2O_2 for 24 h. **C., E.** Cells transfected with or without Nrf2-siRNA or control siRNA were pretreated with 50 μg/ml coptisine for 1 h, and stimulated with or without 0.5 mM H_2O_2 for 24 h. **F.** Cells were pretreated with 50 μg/ml coptisine and/or 10 μM ZnPP for 1 h, and then stimulated with or without 0.5 mM H_2O_2 for 24 h. **A., C.** Cell lysates were subjected to gel electrophoresis, and then Western blot analysis was performed using the indicated antibodies. Actin was used as an internal control. **B., D.** Bands were quantified using ImageJ, normalized to actin and ratios were determined. **E., F.** The cell viability was estimated using an MTT assay (* $p < 0.05$ compared with the control group, # $p < 0.05$ compared with the H_2O_2-treated group, & $p < 0.05$ compared with the coptisine and H_2O_2-treated group).

A

B

C
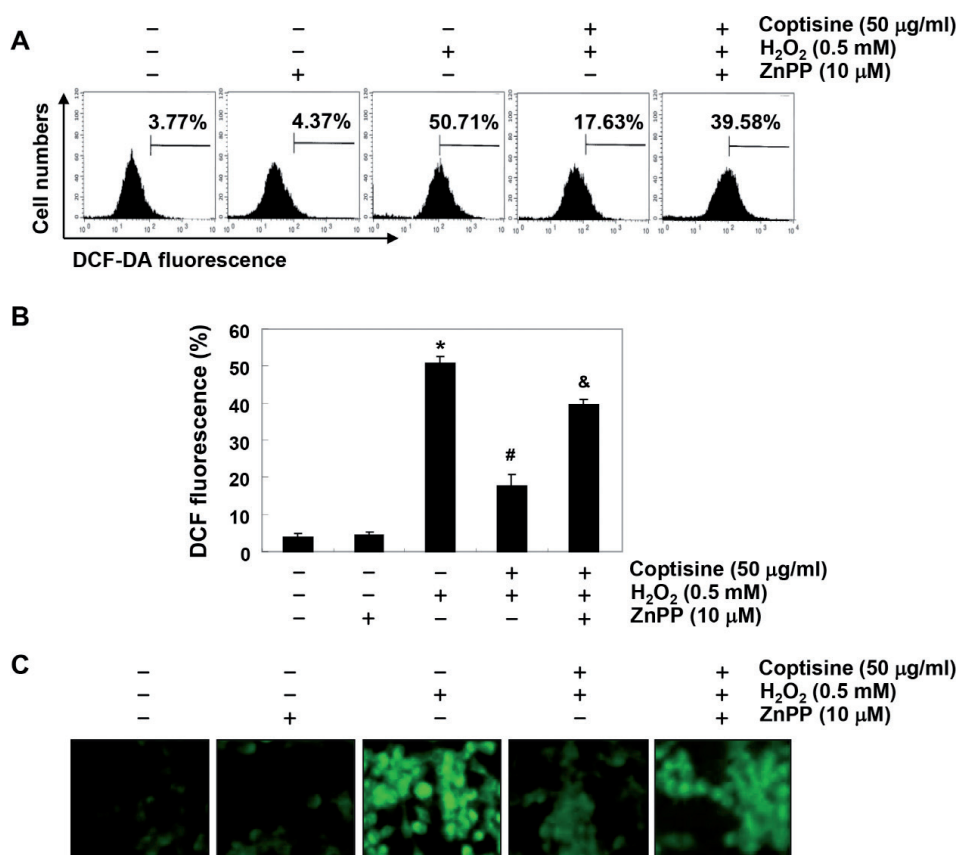
Figure 3. Protection of H_2O_2-induced ROS generation by coptisine in HaCaT cells. Cells were pretreated with 50 μg/ml coptisine and/or 10 μM ZnPP for 1 h, and then stimulated with or without 0.5 mM H_2O_2 for 1 h. **A., B.** After staining with DCF-DA fluorescent dye, DCF fluorescence was monitored by a flow cytometer (* $p < 0.05$ compared with the control group, $^\#$ $p < 0.05$ compared with the H_2O_2-treated group, $^\&$ $p < 0.05$ compared with the coptisine and H_2O_2-treated group). **C.** Images were obtained by a fluorescence microscope (original magnification, 200×).

all of coptisine's protective effect against DNA damage by H_2O_2, suggesting that the cytoprotective effect of coptisine on oxidative stress-induced DNA damage in HaCaT cells is mediated through HO-1 induction.

Coptisine diminished H_2O_2-induced mitochondrial dysfunction in HaCaT keratinocytes

In order to examine the protective effect of coptisine on mitochondrial dysfunction by H_2O_2, MMP and intracellular ATP levels were evaluated. According to the results of JC-1 staining shown in Figures 5A and B, changes in the ratio of polarized and depolarized cell populations were observed in HaCaT cells treated with H_2O_2, and the increase in depolarized mitochondrial membrane was significantly higher than in the control group. In agreement with this result, the concentration of ATP in cells exposed to H_2O_2 was significantly reduced, compared with in cells cultured in normal medium (Figure 5C). However, coptisine was able to prevent these changes, and the protective effects of coptisine were significantly abrogated in the presence of ZnPP, demonstrating that the activation of HO-1 was involved in this protective activity.

Coptisine suppressed H_2O_2-induced apoptosis in HaCaT keratinocytes

DAPI staining, flow cytometry, and agarose gel electrophoresis analyses were further performed, to investigate whether the cytoprotective effect of coptisine against H_2O_2 on HaCaT cells was related to apoptosis suppression. The fluorescent images in Figure 6A reveal that the control cells had intact nuclei, while the H_2O_2-treated cells showed significant chromatin condensation, which is observed in the apoptosis-induced cells. However, the morphological changes were markedly attenuated in the cells pretreated with coptisine before the treatment with H_2O_2. The results of Annexin V/PI double staining also showed that the pretreatment of coptisine significantly decreased the frequency of apoptotic cells in H_2O_2-stimulated cells (Figures 6B and C). In addition, H_2O_2-induced DNA fragmentation, another evidence of the apoptosis induction, was markedly attenuated in cells treated with coptisine prior to H_2O_2 stimulation (Figure 6D). Worth noting, ZnPP also excluded the beneficial effects of coptisine on H_2O_2-induced apoptosis, indicating that the protective role of coptisine was at least dependent on HO-1.

Coptisine restored H_2O_2-induced alteration of the apoptosis regulatory genes in HaCaT keratinocytes

To investigate the mechanisms of apoptosis-protective effect of coptisine and the role of HO-1, the effect of coptisine and ZnPP on H_2O_2-induced changes of apoptosis regulatory genes expression was finally examined. The immunoblotting results of Figures 7A and B show that anti-apoptotic Bcl-2 protein was significantly down-regulated in H_2O_2-treated HaCaT cells, while the pro-apoptotic Bax protein was up-regulated. In addition, the expression of pro-caspase-3 was markedly reduced. However, expression of active caspase-3 was not detected under the same conditions. Thus, the *in vitro* activity of caspase-3 was measured and its activity was

found to be increased about 4-fold in H_2O_2-treated cells compared to the control (Figure 7C), which was associated with the degradation of PARP, a representative substrate protein degraded by activated caspase-3 (Figures 7A and B). However, these changes by H_2O_2 treatment were relatively conservative in the coptisine-pretreated cells, and the protective potentials of coptisine disappeared under the condition in which the activation of HO-1 was suppressed.

Discussion

Overload of intracellular ROS due to the imbalance of ROS production and defense of antioxidant systems can oxidize
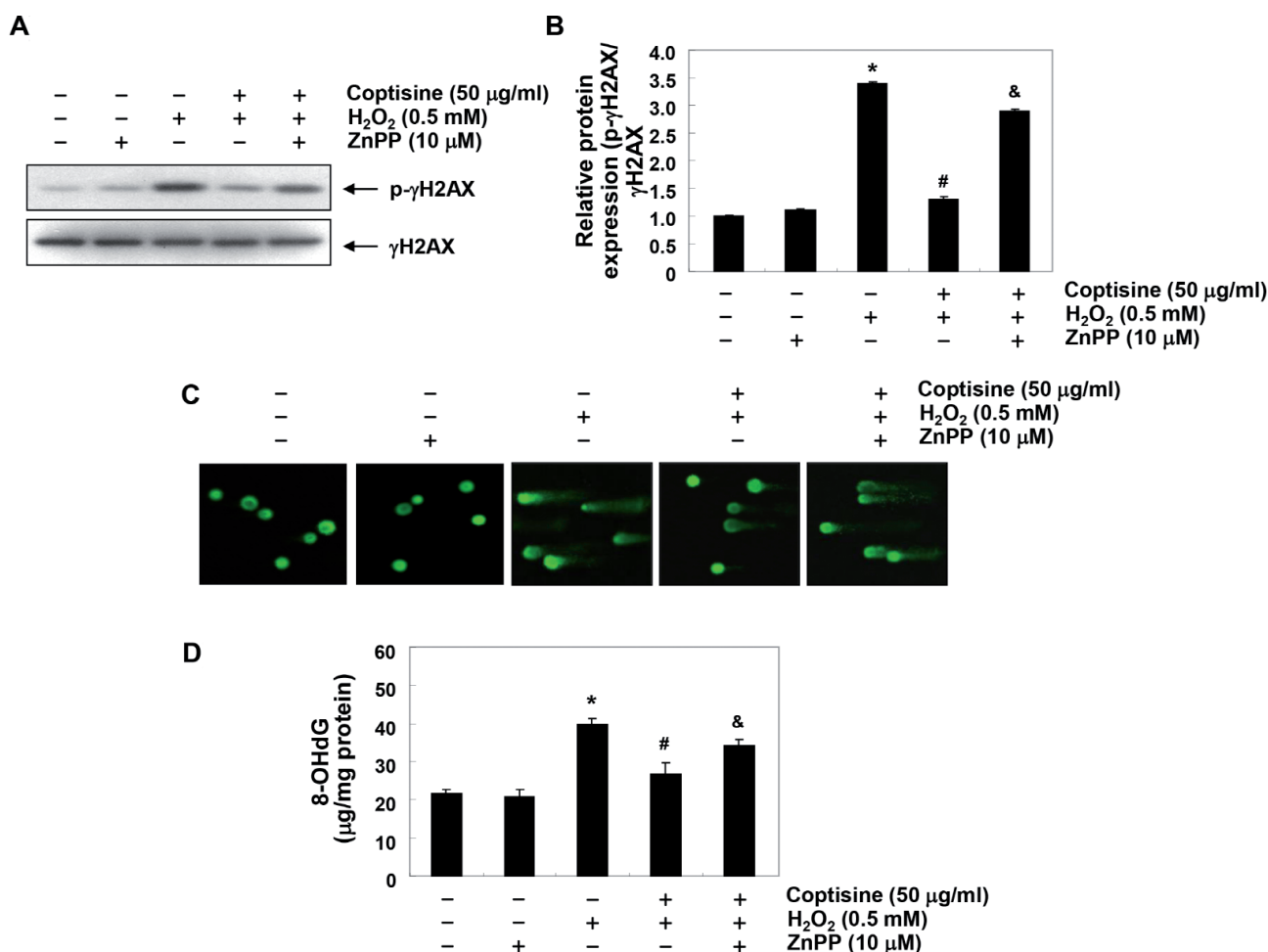
Figure 4. Protection of H_2O_2-induced DNA damage by coptisine in HaCaT cells. Cells were pretreated with 50 µg/ml coptisine and/or 10 µM ZnPP for 1 h, and then stimulated with or without 0.5 mM H_2O_2 for 24 h. **A.** Cell lysates were subjected to gel electrophoresis, and then Western blot analysis was performed using anti-γH2AX and -p-γH2AX antibodies. **B.** Bands were quantified using ImageJ and ratios were determined to the relative values of phosphorylated form relative to the total protein amount of γH2AX. **C.** Comet assay was used to assess DNA damage (original magnification, 200×). **D.** The 8-OHdG content in cellular DNA was measured with an EIA kit (* $p < 0.05$ compared with the control group, # $p < 0.05$ compared with the H_2O_2-treated group, & $p < 0.05$ compared with the coptisine and H_2O_2-treated group).
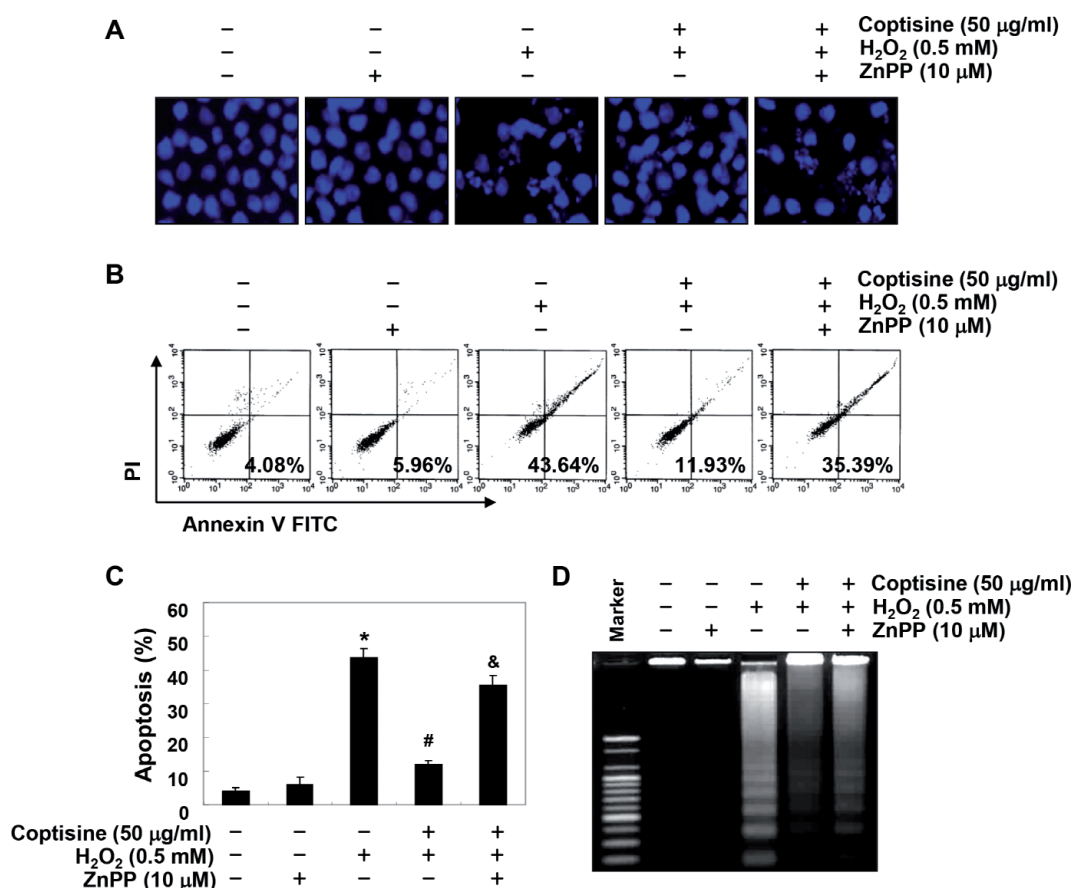
A

B

C
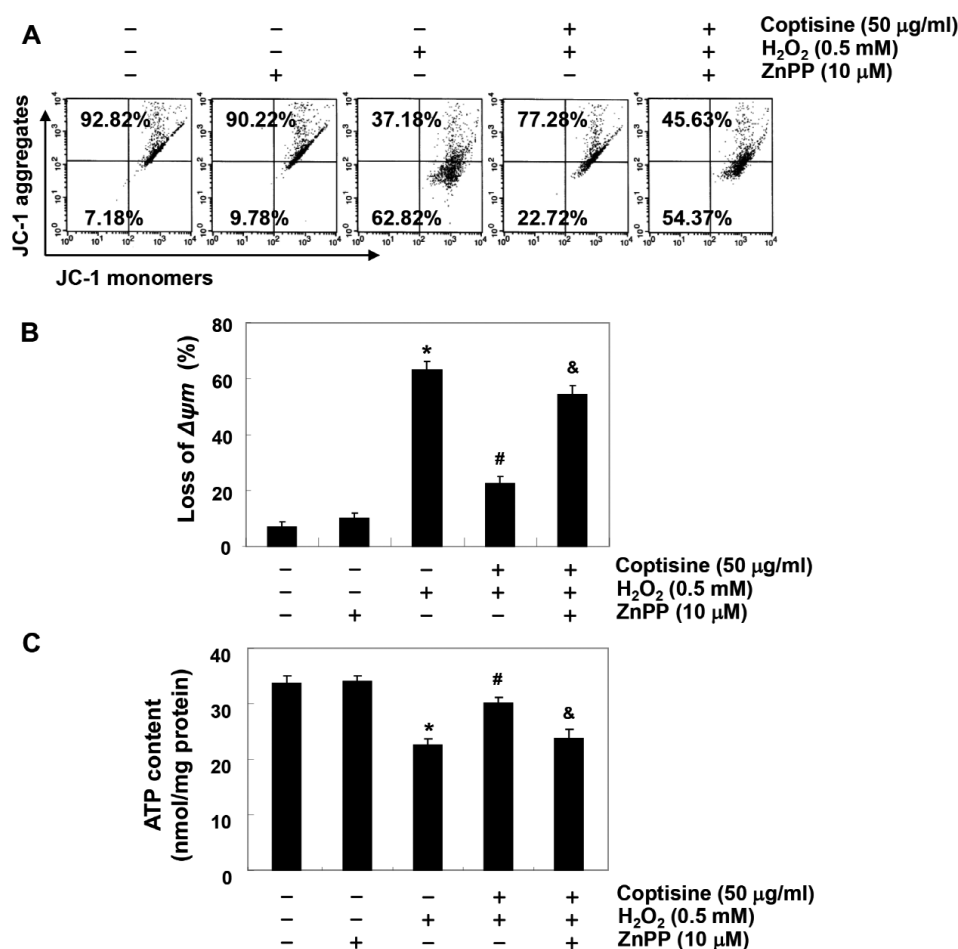
Figure 5. Attenuation of H_2O_2-induced mitochondrial dysfunction by coptisine in HaCaT cells. Cells were pretreated with 50 µg/ml coptisine and/or 10 µM ZnPP for 1 h, and then stimulated with or without 0.5 mM H_2O_2 for 24 h. **A., B.** The values of MMP were evaluated by a flow cytometer (* $p < 0.05$ compared with the control group, # $p < 0.05$ compared with the H_2O_2-treated group, & $p < 0.05$ compared with the coptisine and H_2O_2-treated group). **C.** The ATP contents were measured with a commercially available kit was used (* $p < 0.05$ compared with the control group, # $p < 0.05$ compared with the H_2O_2-treated group, & $p < 0.05$ compared with the coptisine and H_2O_2-treated group).

important components of cells, such as nucleic acids, proteins, and lipids, ultimately leading to oxidative damage (Valko et al. 2016; Treberg et al. 2019). H_2O_2, one of the major ROS, is nonradical 2-electron reduction product of oxygen. Although the concentration of H_2O_2 acting as a messenger molecule varies depending on the cell type (Sies 2014), H_2O_2 dissociates in the cell to form reactive and destructive hydroxyl radicals that contribute to DNA damage and subsequent apoptosis (Rezvani et al. 2007; Piao et al. 2012). Recently, H_2O_2-induced oxidative stress has been shown to induce apoptosis through mitochondrial dysfunction in keratinocytes (Sun et al. 2017; Yoon et al. 2017). Therefore, in this study, exogenous H_2O_2 treatment was selected as an inducer of oxidative damage to HaCaT keratinocytes. The current results demonstrate that coptisine prevented H_2O_2-induced DNA damage and apoptosis of HaCaT keratinocyte through the rescue of mitochondrial function by blocking ROS accumulation. The results also demonstrate that coptisine promoted activation of the Nrf2/HO-1 signaling pathway, and inhibition of HO-1 activity eliminated the protective effect of coptisine, suggesting that

the protective action of coptisine on HaCaT cells was at least Nrf2-mediated HO-1 dependent.

It is well known that Nrf2 is a ubiquitous transcription factor, which plays the role of a central regulator in protecting cells from oxidative damage (Kobayashi and Yamamoto 2005; Lee et al. 2011a; Qiu et al. 2014). Among one of the Nrf2-dependent cytoprotective enzymes, HO-1 plays a critical role in heme catabolism, and produces biliverdin, ferrous iron, and carbon monoxide. This enzyme is also activated in response to various oxidative signals, and provides adaptive and beneficial cellular responses to oxidative damage, not limited to the degradation of toxic heme released by hemoproteins (Kobayashi and Yamamoto 2005; Loboda et al. 2016). The results show that H_2O_2 alone partially increases the expression of HO-1, as well as the expression and phosphorylation of Nrf2, which were further markedly increased by the co-treatment with coptisine, compared to that of the cells treated H_2O_2 alone. However, transient knockdown of Nrf2 with Nrf2-siRNA markedly reduced coptisine-mediated Nrf2 activation and HO-1 induction, which is evidence that the increased HO-1 expression is

Figure 6. Suppression of H_2O_2-induced apoptosis by coptisine in HaCaT cells. Cells were treated with 50 μg/ml coptisine and/or 10 μM ZnPP for 1 h, and then stimulated with or without 0.5 mM H_2O_2 for 24 h. **A.** The DAPI-stained nuclei were observed using a fluorescence microscope (original magnification, 400×). **B., C.** The percentages of apoptotic cells were then analyzed using flow cytometric analysis (* $p < 0.05$ compared with the control group, [#] $p < 0.05$ compared with the H_2O_2-treated group, [&] $p < 0.05$ compared with the coptisine and H_2O_2-treated group). **D.** DNA fragmentation was analyzed by an agarose gel electrophoresis. The results are representative of those obtained from three independent experiments.

mediated by Nrf2. Additionally, transient knockdown of Nrf2 and ZnPP, an HO-1 specific inhibitor, caused the coptisine-induced preventive effects in H_2O_2-induced reduction of cell viability to completely disappear.

Similar to the results of this study, previous studies have shown that H_2O_2 alone can induce the expression of HO-1 (Aggeli et al. 2006; Lee et al. 2011b), and the up-regulation of HO-1 has been identified as a defense mechanism against H_2O_2-induced apoptosis in a variety of cell types, including keratinocytes (Hseu et al. 2015; Yoon et al. 2017; Yang et al. 2018). In addition, overexpression of HO-1 exhibited resistance to DNA damage and apoptosis induced by oxidative stress (Kobayashi and Yamamoto 2005; Hseu et al. 2015; Loboda et al. 2016); however, inhibition of HO-1 activity improved cytotoxicity against oxidative stress, and reduced the efficacy of antioxidants (Hirai et al. 2007; Zhu et al. 2014, 2015). Thus, the effect of ZnPP on the inhibitory

effect of ROS production by coptisine was investigated in H_2O_2-treated HaCaT keratinocytes, and it was observed that ZnPP treatment significantly abolished the beneficial effect of ROS production by coptisine. These results suggest that the protective effect of coptisine on H_2O_2-induced oxidative stress is mediated through the activation of Nrf2/HO-1 signaling. Furthermore, ZnPP significantly diminished the inhibitory effect of coptisine on H_2O_2-induced DNA damage, which also implies that the protective role of coptisine on H_2O_2-induced cytotoxicity was dependent on the HO-1 in HaCaT keratinocytes.

Ample experimental evidence has shown that mitochondria in keratinocytes are the primary intracellular organelle of H_2O_2 toxicity, while excessive accumulation of ROS by oxidative stress is one of the mechanisms leading to apoptosis associated with mitochondrial injury (Sun et al. 2017; Yoon et al. 2017). In addition, HO-1 activation in keratinocytes

is recognized as a cytoprotective mechanism against oxidative stress-mediated mitochondrial dysfunction, through inactivation of the mitochondria-mediated intrinsic apoptosis pathway (Zhu et al. 2014; Hseu et al. 2015; Duan et al. 2016). In the induction of ROS-mediated apoptosis, ROS causes free radical attack of the mitochondrial membrane phospholipid. As a result, mitochondrial membrane depolarization occurs and MMP is lost, which is considered to be an onset of intrinsic apoptosis pathway (Finkel and Holbrook 2000; Rigoulet et al. 2011). At the same time, mitochondrial dysfunction disrupts the production of intracellular ATP, by promoting abnormalities in the electron transport pathway of the mitochondrial respiratory chain (D'Autréaux et al. 2007; Valero 2014). Ultimately, intracellular ATP levels can be used as an indicator of the homeostasis of mitochondrial energy metabolism (Orrenius 2007; Cui et al. 2017). The current studies show that when cells were exposed to H_2O_2, MMP levels and ATP contents were significantly reduced compared to controls, whereas coptisine reversed the loss of MMP and APT by H_2O_2. However, in the presence of ZnPP, coptisine-mediated repair of mitochondrial dysfunction and

decrease of ATP production were significantly abolished. In view of maintaining energy homeostasis, these results are in good agreement with previous studies that show that the protective effect of apoptosis on oxidative stress is related to the maintenance of ATP production by the preservation of mitochondrial function (Mao et al. 2014; Tian et al. 2017). Therefore, the conservation of ATP production by the maintenance of mitochondrial function is considered to be a possible mechanism by which coptisine can preserve keratinocyte survival pathway from oxidative stress through HO-1 activation.

The activation of apoptosis through caspase cascade is regulated by various proteins, including Bcl-2 family members that consist of anti-apoptotic and pro-apoptotic proteins. Among the Bcl-2 family members, anti-apoptotic proteins, such as Bcl-2, are located on the outer mitochondrial membrane to prevent the release of apoptogenic factors, and provide protection by inhibiting the consumption of ATP (Gustafsson and Gottlieb 2007; Kiraz et al. 2016). On the other hand, pro-apoptotic proteins, including Bax, antagonize anti-apoptotic proteins, or translocate to mitochondrial
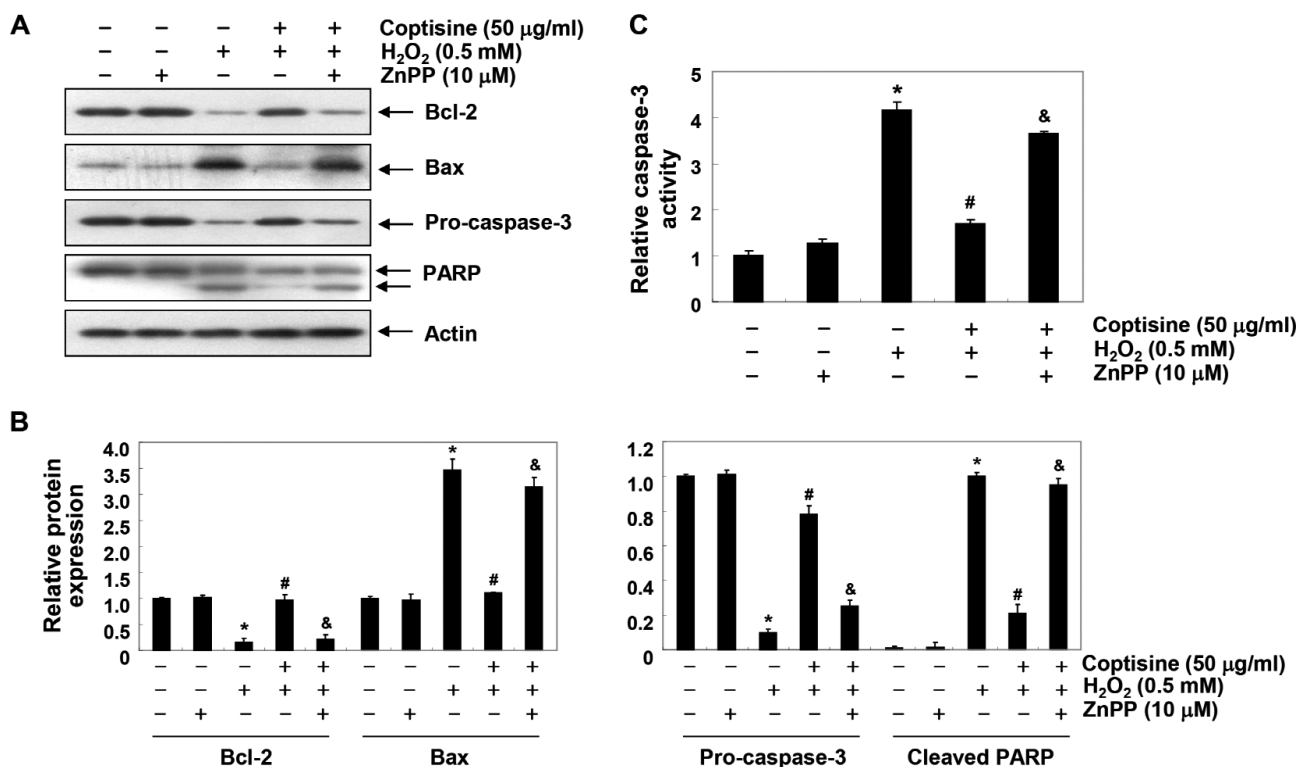
Figure 7. Effect of coptisine on the expression of apoptosis regulatory genes in H_2O_2-treated HaCaT cells. **A., B.** After treatment with 50 μg/ml coptisine and/or 10 μM ZnPP in the presence or absence of 0.5 mM H_2O_2 for 24 h, the cellular proteins were subjected to gel electrophoresis, and then Western blot analysis was performed using the indicated antibodies. Actin was used as an internal control. **B.** Bands were quantified using ImageJ, normalized to actin and ratios were determined. **C.** The caspase-3 activity was measured using an ELISA microplate reader (* $p < 0.05$ compared with the control group, [#] $p < 0.05$ compared with the H_2O_2-treated group, [&] $p < 0.05$ compared with the coptisine and H_2O_2-treated group).

membranes to form membrane-integrated homo oligomers that induce mitochondrial pore formation, leading to the loss of MMP, resulting in the cytosolic release of apoptogenic factors (Imahashi et al. 2004; Kulikov et al. 2012). Thus, the balance of apoptotic Bax family proteins to anti-apoptotic Bcl-2 family proteins serves as a determinant to induce or inhibit the initiation of the intrinsic apoptosis pathway. Many previous studies have shown that the induction of apoptosis by H_2O_2 in keratinocytes was associated with a decrease in the Bcl-2/Bax ratio and/or activation of caspases (Kanda and Watanabe 2003; Sun et al. 2017). The present results show that the presence of coptisine reversed the decreased expression of Bcl-2, and increased the expression of Bax observed in H_2O_2-treated HaCaT keratinocytes. In addition, coptisine administration blocked the H_2O_2-induced activation of caspase-3, and the degradation of PARP, concomitant with reduced apoptosis. In this respect, it is suggested that coptisine can rescue H_2O_2-induced cytotoxic injury by blocking mitochondria-mediated apoptosis. However, the inhibition of HO-1 function using an HO-1 inhibitor markedly hindered these protective effects. These results are in good agreement with other recent studies that show that HO-1 restored cell survival through the prevention of oxidative damage-mediated apoptosis (Yu et al. 2013; Chen et al. 2017; Zhang et al. 2018), indicating that the cellular protective potential of coptisine against oxidative stress in HaCaT keratinocytes is at least dependent on the activation of Nrf2/HO-1 signaling.

In summary, the current study demonstrates that coptisine can effectively protect HaCaT keratinocytes from H_2O_2-induced cytotoxicity, by blocking oxidative stress-mediated DNA damage and mitochondria-dependent apoptotic pathway, through Nrf2/HO-1 signaling-mediated antioxidant action. Although studies on mitochondrial damage-associated energy metabolism and its associated signal molecules are needed, the present findings may be presented as evidence that coptisine can alter the redox state of keratinocytes, and thereby regulate cellular antioxidant signaling pathways.

Conflict of interest: The author has no conflict of interest to declare.

References

Aggeli IK, Gaitanaki C, Beis I (2006): Involvement of JNKs and p38-MAPK/MSK1 pathways in H2O2-induced upregulation of heme oxygenase-1 mRNA in H9c2 cells. Cell. Signal. **18,** 1801-1812
https://doi.org/10.1016/j.cellsig.2006.02.001

Chen H, Tang X, Zhou B, Zhou Z, Xu N, Wang Y (2017): A ROS-mediated mitochondrial pathway and Nrf2 pathway activation are involved in BDE-47 induced apoptosis in Neuro-2a cells. Chemosphere **184,** 679-686
https://doi.org/10.1016/j.chemosphere.2017.06.006

Cheng CF, Zerzan JC, Johnson DB, Juul SE (2012): Zinc protoporphyrin-to-heme ratios in high-risk and preterm infants. J. Pediatr. **161,** 81-87
https://doi.org/10.1016/j.jpeds.2011.12.048

Cho EJ, Yokozawa T, Rhee SH, Park KY (2004): The role of Coptidis Rhizoma extract in a renal ischemia-reperfusion model. Phytomedicine **11,** 576-584
https://doi.org/10.1016/j.phymed.2003.07.005

Cui L, Li Z, Chang X, Cong G, Hao L (2017): Quercetin attenuates vascular calcification by inhibiting oxidative stress and mitochondrial fission. Vascul. Pharmacol. **88,** 21-29
https://doi.org/10.1016/j.vph.2016.11.006

D'Autréaux B, Toledano MB (2007): ROS as signalling molecules: mechanisms that generate specificity in ROS homeostasis. Nat. Rev. Mol. Cell. Biol. **8,** 813-824
https://doi.org/10.1038/nrm2256

D'Errico M, Lemma T, Calcagnile A, Proietti De Santis L, Dogliotti E (2007): Cell type and DNA damage specific response of human skin cells to environmental agents. Mutat. Res. **614,** 37-47
https://doi.org/10.1016/j.mrfmmm.2006.06.009

Duan X, Li J, Li W, Xing X, Zhang Y, Li W, Zhao L, Sun G, Gao XH, Li B (2016): Antioxidant tert-butylhydroquinone ameliorates arsenic-induced intracellular damages and apoptosis through induction of Nrf2-dependent antioxidant responses as well as stabilization of anti-apoptotic factor Bcl-2 in human keratinocytes. Free Radic. Biol. Med. **94,** 74-87
https://doi.org/10.1016/j.freeradbiomed.2016.02.009

Fang J, Seki T, Maeda H (2009): Therapeutic strategies by modulating oxygen stress in cancer and inflammation. Adv. Drug Deliv. Rev. **61,** 290-302
https://doi.org/10.1016/j.addr.2009.02.005

Finkel T, Holbrook NJ (2000): Oxidants, oxidative stress and the biology of ageing. Nature **408,** 239-247
https://doi.org/10.1038/35041687

Gong LL, Fang LH, Wang SB, Sun JL, Qin HL, Li XX, Wang SB, Du GH (2012): Coptisine exert cardioprotective effect through anti-oxidative and inhibition of RhoA/Rho kinase pathway on isoproterenol-induced myocardial infarction in rats. Atherosclerosis **222,** 50-58
https://doi.org/10.1016/j.atherosclerosis.2012.01.046

Gustafsson AB, Gottlieb RA (2007): Bcl-2 family members and apoptosis, taken to heart. Am. J. Physiol. Cell. Physiol. **292,** C45-51
https://doi.org/10.1152/ajpcell.00229.2006

Hirai K, Sasahira T, Ohmori H, Fujii K, Kuniyasu H (2007): Inhibition of heme oxygenase-1 by zinc protoporphyrin IX reduces tumor growth of LL/2 lung cancer in C57BL mice. Int. J. Cancer **120,** 500-505
https://doi.org/10.1002/ijc.22287

Hjortsø MD, Andersen MH (2014): The expression, function and targeting of haem oxygenase-1 in cancer. Curr. Cancer Drug Targets **14,** 337-347
https://doi.org/10.2174/1568009614666140320111306

Hseu YC, Lo HW, Korivi M, Tsai YC, Tang MJ, Yang HL (2015): Dermato-protective properties of ergothioneine through induction of Nrf2/ARE-mediated antioxidant genes in UVA-irradiated human keratinocytes. Free Radic. Biol. Med. **86,** 102-117
https://doi.org/10.1016/j.freeradbiomed.2015.05.026

Hu YR, Ma H, Zou ZY, He K, Xiao YB, Wang Y, Feng M, Ye XL, Li XG (2017): Activation of Akt and JNK/Nrf2/NQO1 pathway contributes to the protective effect of coptisine against AAPH-induced oxidative stress. Biomed. Pharmacother. **85,** 313-322
https://doi.org/10.1016/j.biopha.2016.11.031

Imahashi K, Schneider MD, Steenbergen C, Murphy E (2004): Transgenic expression of Bcl-2 modulates energy metabolism, prevents cytosolic acidification during ischemia, and reduces ischemia/reperfusion injury. Circ. Res. **95,** 734-741
https://doi.org/10.1161/01.RES.0000143898.67182.4c

Jang MH, Kim HY, Kang KS, Yokozawa T, Park JH (2009): Hydroxyl radical scavenging activities of isoquinoline alkaloids isolated from Coptis chinensis. Arch. Pharm. Res. **32,** 341-345
https://doi.org/10.1007/s12272-009-1305-z

Jung HA, Min BS, Yokozawa T, Lee JH, Kim YS, Choi JS (2009): Anti-Alzheimer and antioxidant activities of Coptidis Rhizoma alkaloids. Biol. Pharm. Bull. **32,** 1433-1438
https://doi.org/10.1248/bpb.32.1433

Kanda N, Watanabe S (2003): 17beta-estradiol inhibits oxidative stress-induced apoptosis in keratinocytes by promoting Bcl-2 expression. J. Invest. Dermatol. **121,** 1500-1509
https://doi.org/10.1111/j.1523-1747.2003.12617.x

Kim MY, Choi EO, HwangBo H, Kwon DH, Ahn KI, Kim HJ, Ji SY, Hong SH, Jeong JW, Kim GY, Park C, Choi YH (2018): Reactive oxygen species-dependent apoptosis induction by water extract of Citrus unshiu peel in MDA-MB-231 human breast carcinoma cells. Nutr. Res. Pract. **12,** 129-134
https://doi.org/10.4162/nrp.2018.12.2.129

Kiraz Y, Adan A, Kartal Yandim M, Baran Y (2016): Major apoptotic mechanisms and genes involved in apoptosis. Tumour Biol. **37,** 8471-8486
https://doi.org/10.1007/s13277-016-5035-9

Kobayashi M, Yamamoto M (2005): Molecular mechanisms activating the Nrf2-Keap1 pathway of antioxidant gene regulation. Antioxid. Redox Signal. **7,** 385-394
https://doi.org/10.1089/ars.2005.7.385

Kulikov AV, Shilov ES, Mufazalov IA, Gogvadze V, Nedospasov SA, Zhivotovsky B (2012): Cytochrome c: the Achilles' heel in apoptosis. Cell. Mol. Life Sci. **69,** 1787-1797
https://doi.org/10.1007/s00018-011-0895-z

Kulms D, Schwarz T (2002): Independent contribution of three different pathways to ultraviolet-B-induced apoptosis. Biochem. Pharmacol. **64,** 837-841
https://doi.org/10.1016/S0006-2952(02)01146-2

Kuribayashi K, Iida S, Nakajima Y, Funaguchi N, Tabata C, Fukuoka K, Fujimori Y, Ihaku D, Nakano T (2015): Suppression of heme oxygenase-1 activity reduces airway hyperresponsiveness and inflammation in a mouse model of asthma. J. Asthma **52,** 662-668
https://doi.org/10.3109/02770903.2015.1008138

Lee SE, Jeong SI, Kim GD, Yang H, Park CS, Jin YH, Park YS (2011a): Upregulation of heme oxygenase-1 as an adaptive mechanism for protection against crotonaldehyde in human umbilical vein endothelial cells. Toxicol. Lett. **201,** 240-248
https://doi.org/10.1016/j.toxlet.2011.01.006

Lee SE, Jeong SI, Yang H, Park CS, Jin YH, Park YS (2011b): Fisetin induces Nrf2-mediated HO-1 expression through PKC-δ and

p38 in human umbilical vein endothelial cells. J. Cell. Biochem. **112,** 2352-2360
https://doi.org/10.1002/jcb.23158

Loboda A, Damulewicz M, Pyza E, Jozkowicz A, Dulak J (2016): Role of Nrf2/HO-1 system in development, oxidative stress response and diseases: an evolutionarily conserved mechanism. Cell. Mol. Life Sci. **73,** 3221-3247
https://doi.org/10.1007/s00018-016-2223-0

Luo JF, Shen XY, Lio CK, Dai Y, Cheng CS, Liu JX, Yao YD, Yu Y, Xie Y, Luo P, Yao XS, Liu ZQ, Zhou H (2018): Activation of Nrf2/HO-1 pathway by nardochinoid C inhibits inflammation and oxidative stress in lipopolysaccharide-stimulated macrophages. Front. Pharmacol. **9,** 911
https://doi.org/10.3389/fphar.2018.00911

Mao CY, Lu HB, Kong N, Li JY, Liu M, Yang CY, Yang P (2014): Levocarnitine protects H9c2 rat cardiomyocytes from H2O2-induced mitochondrial dysfunction and apoptosis. Int. J. Med. Sci. **11,** 1107-1115
https://doi.org/10.7150/ijms.9153

Meng FC, Wu ZF, Yin ZQ, Lin LG, Wang R, Zhang QW (2018): Coptidis rhizoma and its main bioactive components: recent advances in chemical investigation, quality evaluation and pharmacological activity. Chin. Med. **13,** 13
https://doi.org/10.1186/s13020-018-0171-3

Orrenius S (2007): Reactive oxygen species in mitochondria-mediated cell death. Drug Metab. Rev. **39,** 443-455
https://doi.org/10.1080/03602530701468516

Park C, Hong SH, Shin SS, Lee DS, Han MH, Cha HJ, Kim S, Kim HS, Kim GY, Park EK, Jeon YJ, Choi YH (2018): Activation of the Nrf2/HO-1 signaling pathway contributes to the protective effects of Sargassum serratifolium extract against oxidative stress-induced DNA damage and apoptosis in SW1353 human chondrocytes. Int. J. Environ. Res. Public Health **15,** E1173
https://doi.org/10.3390/ijerph15061173

Piao MJ, Zhang R, Lee NH, Hyun JW (2012): Protective effect of triphlorethol-A against ultraviolet B-mediated damage of human keratinocytes. J. Photochem. Photobiol. B **106,** 74-80
https://doi.org/10.1016/j.jphotobiol.2011.10.007

Qiu L, Song Z, Setaluri V (2014): Oxidative stress and vitiligo: the Nrf2-ARE signaling connection. J. Invest. Dermatol. **134,** 2074-2076
https://doi.org/10.1038/jid.2014.241

Rezvani HR, Cario-André M, Pain C, Ged C, deVerneuil H, Taïeb A (2007): Protection of normal human reconstructed epidermis from UV by catalase overexpression. Cancer Gene Ther. **14,** 174-186
https://doi.org/10.1038/sj.cgt.7701000

Rigoulet M, Yoboue ED, Devin A (2011): Mitochondrial ROS generation and its regulation: mechanisms involved in H2O2 signaling. Antioxid. Redox Signal. **14,** 459-468
https://doi.org/10.1089/ars.2010.3363

Sies H (2014): Role of metabolic H2O2 generation: redox signaling and oxidative stress. J. Biol. Chem. **289,** 8735-8741
https://doi.org/10.1074/jbc.R113.544635

Sosa V, Moliné T, Somoza R, Paciucci R, Kondoh H, LLeonart ME (2013): Oxidative stress and cancer: an overview. Ageing Res. Rev. **12,** 376-390
https://doi.org/10.1016/j.arr.2012.10.004

Sun Y, Zhou C, Huang S, Jiang C (2017): Selenium polysaccharide SPMP-2a from Pleurotus geesteranus alleviates H2O2-induced oxidative damage in HaCaT cells. Biomed. Res. Int. **2017,** 4940384
https://doi.org/10.1155/2017/4940384

Tian X, He W, Yang R, Liu Y (2017): Dl-3-n-butylphthalide protects the heart against ischemic injury and H9c2 cardiomyoblasts against oxidative stress: involvement of mitochondrial function and biogenesis. J. Biomed. Sci. **24,** 38
https://doi.org/10.1186/s12929-017-0345-9

Treberg JR, Braun K, Selseleh P (2019): Mitochondria can act as energy-sensing regulators of hydrogen peroxide availability. Redox Biol. **20,** 483-488
https://doi.org/10.1016/j.redox.2018.11.002

Valero T (2014): Mitochondrial biogenesis: pharmacological approaches. Curr. Pharm. Des. **20,** 5507-5509
https://doi.org/10.2174/138161282035140911142118

Valko M, Jomova K, Rhodes CJ, Kuča K, Musílek K (2016): Redox- and non-redox-metal-induced formation of free radicals and their role in human disease. Arch. Toxicol. **90,** 1-37
https://doi.org/10.1007/s00204-015-1579-5

Xu Z, Feng W, Shen Q, Yu N, Yu K, Wang S, Chen Z, Shioda S, Guo Y (2017): Rhizoma coptidis and berberine as a natural drug to combat aging and aging-related diseases via anti-oxidation and AMPK activation. Aging Dis. **8,** 760-777
https://doi.org/10.14336/AD.2016.0620

Yang HL, Lee CL, Korivi M, Liao JW, Rajendran P, Wu JJ, Hseu YC (2018): Zerumbone protects human skin keratinocytes against UVA-irradiated damages through Nrf2 induction. Biochem. Pharmacol. **148,** 130-146
https://doi.org/10.1016/j.bcp.2017.12.014

Yokozawa T, Ishida A, Kashiwada Y, Cho EJ, Kim HY, Ikeshiro Y (2004): Coptidis Rhizoma: protective effects against peroxyni-trite-induced oxidative damage and elucidation of its active components. J. Pharm. Pharmacol. **56,** 547-556
https://doi.org/10.1211/0022357023024

Yoon JJ, Jeong JW, Choi EO, Kim MJ, Hwang-Bo H, Kim HJ, Hong SH, Park C, Lee DH, Choi YH (2017): Protective effects of Scutellaria baicalensis Georgi against hydrogen peroxide-induced DNA damage and apoptosis in HaCaT human skin keratinocytes. EXCLI J. **16,** 426-438

Yu J, Zhu X, Qi X, Che J, Cao B (2013): Paeoniflorin protects human EA.hy926 endothelial cells against gamma-radiation induced oxidative injury by activating the NF-E2-related factor 2/heme oxygenase-1 pathway. Toxicol. Lett. **218,** 224-234
https://doi.org/10.1016/j.toxlet.2013.01.028

Zhang XT, Sun XQ, Wu C, Chen JL, Yuan JJ, Pang QF, Wang ZP (2018): Heme oxygnease-1 induction by methylene blue protects RAW264.7 cells from hydrogen peroxide-induced injury. Biochem. Pharmacol. **48,** 265-277
https://doi.org/10.1159/000139189

Zhu W, Xu J, Ge Y, Cao H, Ge X, Luo J, Xue J, Yang H, Zhang S, Cao J (2014): Epigallocatechin-3-gallate (EGCG) protects skin cells from ionizing radiation via heme oxygenase-1 (HO-1) overexpression. J. Radiat. Res. **55,** 1056-1065
https://doi.org/10.1093/jrr/rru047

Zhu XF, Li W, Ma JY, Shao N, Zhang YJ, Liu RM, Wu WB, Lin Y, Wang SM (2015): Knockdown of heme oxygenase-1 promotes apoptosis and autophagy and enhances the cytotoxicity of doxorubicin in breast cancer cells. Oncol. Lett. **10,** 2974-2980
https://doi.org/10.3892/ol.2015.3735